*Mechanical Engineering Advances 2023; 1(1): 106.*
Original Research Article

# Analysing entropy generation of MHD (50:50) slip flow over an inclined needle

**Selvaraj Priya[1], Gundada Raju Rajamani[1], Bhose Ganga[2], Abdul Kaffoor Abdul Hakeem[1,*], Pachiyappan Ragupathi[1,*]**

[1] *Department of Mathematics, Sri Ramakrishna Mission Vidyalaya College of Arts and Science, Coimbatore 641020, India*

[2] *Department of Mathematics, Providence College for Women, Coonoor 643104, India*

*** Corresponding authors:** Abdul Kaffoor Abdul Hakeem, drabdulmaths@gmail.com; Pachiyappa Ragupathi, ragupathiprs@gmail.com

**ARTICLE INFO**

Received: 3 July 2023
Accepted: 16 August 2023
Available online: 19 September 2023

doi: 10.59400/mea.v1i1.106

Copyright © 2023 Author(s).

*Mechanical Engineering Advances* is published by Academic Publishing Pte. Ltd. This article is licensed under the Creative Commons Attribution License (CC BY 4.0).
https://creativecommons.org/licenses/by/4.0/

**ABSTRACT:** The primary objective of this study is to quantify the rate of entropy generation within the magnetohydrodynamic (MHD) slip flow system over the inclined needle. Entropy generation is a measure of the irreversibility and inefficiency in the flow process. The slip flow condition at the fluid interface can significantly impact the flow characteristics and heat transfer rates. In the hybrid nanofluid flow, which consists of non-magnetic and magnetic ($Al_2O_3$ and $Fe_3O_4$) nanoparticles, $H_2O + C_2H_6O_2$ (50:50) are considered as the base fluid. Furthermore, the effects of inclined magnetic fields are taken into interpretation. The PDE's governing equations are converted into ODE's using similarity transformations and solved by a numerical technique based on BVP4C. The results illustrate that crucial parameters such as the magnetic parameter, mixed convection parameter, nanoparticles of solid volume fractions, and Prandtl numbers are pointedly impacted by momentum and thermal profiles. The entropy and Bejan number also consider being various relationship-combined parameters. These analyses protest that raising the magnetic parameter estates an increase in the hybrid nanofluid thermal profile under slip circumstances. Examined magnetic field impact on flow and entropy generation in MHD flows, revealing significant changes in entropy generation due to interaction between magnetic field and nanoparticles. This analysis understands the impact of MHD and slip effects on entropy generation, particularly in the context of the newly emerging 50:50 fluid mixture. Hybrid nanofluids have been shown to have improved thermal conductivity compared to traditional fluids, which can enhance the cooling or heating capabilities of the inclined needle.

***KEYWORDS:*** inclined needle; heat transfer; hybrid nanofluid; entropy generation; Bejan number

## 1. Introduction

Hybrid nanofluids can significantly enhance heat transfer properties compared to traditional heat transfer fluids. The combination of nanoparticles with distinct thermal conductivities can lead to improved cooling efficiency in various systems, such as heat exchangers, electronic devices, and power plants. This research analyzes an inclined surface; the gravitational force acts as an additional driving

force, influencing the flow behavior. If the gravitational force component parallel to the inclined surface exceeds the yield stress of the material, the material will start to flow downhill[1]. This research analyzes the understanding of these dynamics, which is crucial for various engineering and environmental applications and requires careful consideration of factors such as viscosity, particle characteristics, and channel inclination[2]. A vertical thin needle in porous medium offers a mathematical framework for analyzing heat and mass transfer rates, enabling researchers and engineers to optimize designs and make informed decisions[3]. Nanofluids are colloidal suspensions with nanoparticles dispersed in base fluids like water, oil, or ethylene glycol. These unique properties significantly improve the thermal conductivity of the base fluid. Enhancing the thermal conductivity of fluids using nanoparticles is a process known as nanofluid technology. This research improved thermal properties, making them promising candidates for enhancing heat transfer efficiency and improving the overall performance of thermal systems[4]. This research analysis identifies the most influential parameters and their impact on the system's behavior. This can help optimize the system design or suggest areas for further research[5,6]. This review analyzes numerical simulations on lid-driven cavity flow with nanofluids, providing valuable insights for researchers and engineers seeking to understand the complexities and potential applications of nanofluid flows in lid-driven cavities[7]. The study examines magnetic separation and filtration processes in industries like wastewater treatment and mining, utilizing nanoparticle magnetization for efficient fluid flow manipulation and control[8]. This study explores magnetic field-electrically conductive fluid interactions, affecting heat and mass transfer in magnetic drug targeting and hyperthermia cancer treatment applications[9]. This study examines non-Fourier heat flux, ferromagnetic properties, and autocatalytic chemical reactions for understanding thermal and dynamical behavior in complex systems, including magnetic fluids[10]. This research analyzes bioconvection, the collective movement of living microorganisms in fluids, particularly nanofluids. Bioconvection can enhance heat transfer and improve the thermal performance of nanofluids, such as bacteria and algae[11]. Investigated in this study are nanoparticle materials like metal oxides, carbon-based materials, and ferromagnetic nanoparticles for optimizing viscous dissipation in cooling systems and microfluidic devices[12]. Recent research in the field of hybrid nanofluids is ongoing, and new applications continue to emerge as scientists explore their unique properties and potential in various fields. This research analyzes Lorentz force and viscous dissipation to predict propylene glycol-water mixture behavior, optimizing system design, controlling fluid flow, and enhancing heat transfer and transport efficiency[13]. This study investigates the effects of natural convection, micropolar hybrid nanofluid, needle orientation, and boundary heating conditions on heat transfer, fluid flow patterns, and temperature distribution in a thin needle[14]. This research investigated stratification in nanoliquids, examining the impact on fluid dynamics and microorganism behavior, potentially affecting bioconvection patterns and gyrotactic microorganism behavior[15,16]. The research examined stretching parameters' impact on fluid flow and heat transfer characteristics, focusing on non-linear profiles in parabolic shapes for realistic scenarios and practical applications[17]. MHD refers to the study of the behavior of electrically conducting fluids in the presence of magnetic fields. The utilization of hybrid nanofluids in MHD systems aims to improve their performance, efficiency, and control. Some of the recent research in this area has focused on investigating the effects of different factors, such as nanoparticle concentration, fluid flow rate, and geometrical shapes, on the overall performance of MHD systems. In recent years, researchers have been investigating the application of hybrid nanofluids in MHD systems with different geometrical shapes. Some of the research areas are following, wedges[18], curve[19], vertical plate[20], sphere[21], flexible walls[22], sinusoidal walls[23]. This research investigates slip effects, which refer to the motion of the fluid near the surface, where the fluid

molecules slip along the solid boundary instead of adhering to it. The findings of such studies can provide valuable insights into the design and optimization of various engineering systems and processes involving heat and mass transfer[24]. Investigated the behavior of nanoparticles in the nanofluid near the wavy cylinder and understood their potential aggregation or settling tendencies due to the presence of the magnetic field[25]. This study investigates the exact and specific results that would depend on the assumptions, boundary conditions, and modelling approaches used in the study. Therefore, the findings may vary across different research works and experimental setups[26]. Researchers have investigated this study is the use of reversible chemical reactions to store and release heat, which is crucial for renewable energy integration and grid stabilization[27]. How the combination of thermal radiation and shear-thinning behavior impacts the overall heat transfer rate in the system is investigated and analyzed[28]. This study examines activation energy, a crucial parameter in nanofluids, which influences chemical reactions and thermal behavior, focusing on energy barriers and their impact on chemical reactions[29]. Studies have investigated the dynamics of the melting front in nanofluids, analyzing how nanoparticles affect the solid-liquid interface and the overall melting process[30]. Recent research may have focused on investigating the impact of different types of nanoparticles, their concentrations, and fluid compositions on entropy generation. Studies may have explored the behavior of hybrid nanofluids in specific applications, such as heat exchangers, refrigeration systems, or power generation. Some studies have shown that the use of hybrid nanofluids can lead to reduced entropy generation compared to traditional fluids. The enhanced thermal conductivity of nanofluids allows for improved heat transmission, reducing the temperature gradients and associated entropy generation. Some of the following recent research is based on entropy generation[31–37].

The main aim of this paper is to use slip flow conditions at the inclined needle, and the impact of the inclined magnetic field needs to be considered. To calculate analytical results, scattering shooting techniques can be used to obtain solutions for velocity, temperature, and other relevant variables. In MHD slip flow, the slip boundary conditions are applied at the fluid interface, and the presence of nanoparticles needs to be considered. These models may include the Brownian motion and thermophoresis effects on nanoparticles. Thermal convection refers to the process of heat transmission in fluids due to the combined effect of buoyancy and fluid motion. The application of a Lorentz force can influence fluid stream and heat transmission processes through magnetohydrodynamics (MHD). The outcomes of this research can provide insights into the thermodynamic efficiency of the system, the impression of slip flow and nanofluid on entropy creation, and the influence of the magnetic field. This information can be useful for optimizing the design and operation of MHD systems utilizing hybrid nanofluids in slip flow conditions with horizontal needle geometries. Entropy generation and the Bejan number are essential concepts in thermodynamics and fluid mechanics. Hybrid nanofluids can potentially improve the performance and efficiency of the needle. Another potential application is in enhancing the heat transmission properties of the needle.

## 2. Mathematical formulation

- For the research, stable, an incompressible 2D axisymmetric dissipative hybrid fluid flow was applied to a moving object with an inclined magnetic field.
- The fluid was composed of $H_2O + C_2H_6O_2(50-50) + Al_2O_3 + Fe_3O_4$.
- The magnetic field intensity applied normally towards the needle is decided by $B = B(x) = \frac{B_0}{\sqrt{x}}$, $T_\infty$ *and* $T_w$ were chosen to represent ambient, surface temperatures.
- The needle passages in a similar or conflicting way as the constant velocity $U_w$ normal with free

continual velocity $U_\infty$ and the flow pattern is shown in **Figure 1**. **Table 1** determines the status of magnetic and nonmagnetic nanoparticle thermophysical properties, as well as hybrid nanofluid thermal properties.

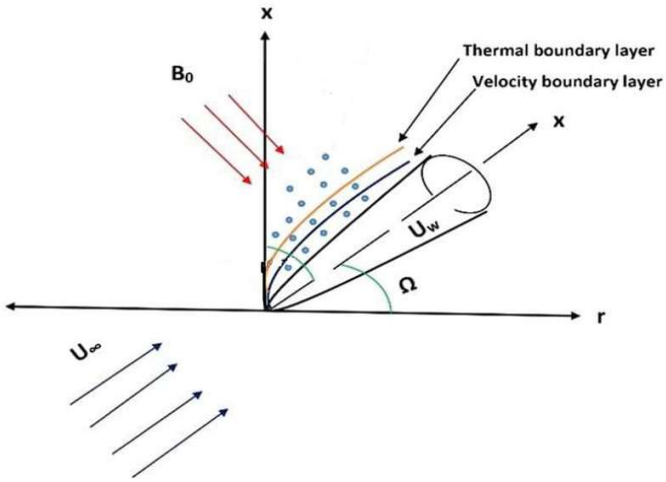


**Figure 1.** Stream outline of contemporary problem.

**Table 1.** Thermophysical characteristics attributes of solid volume fractions of nanoparticles and base fluid[5,6].

| **Attributes** | $\mathbf{Al_2O_3}$ | $\mathbf{Fe_3O_4}$ | $\mathbf{H_2O + C_2H_6O_2\ (50:50)}$ |
|---|---|---|---|
| Density (kg/m$^3$) | 3970 | 5180 | 1067.5 |
| Specific heat (j/kg/k) | 765 | 670 | 3300 |
| Thermal conductivity (w m k) | 9.7 | 40 | 0.3799 |
| Dynamic viscosity (kg/ms) | - | - | 0.00339 |
| Thermal expansion $\beta/10^{-5}(1/k)$ | 0.85 | 1.3 | 58 |

These conventions allow for the specification of flow controlling equations as[13]

Continuity equation:

$$r(u)_x + r(v)_r = 0 \tag{1}$$

Momentum equation:

$$uu_x + vu_r = \frac{\mu_{hnf}}{\rho_{hnf}}\left(\frac{1}{r}\right)(ru_r)_r - u\frac{\sigma B^2}{\rho_{hnf}}\sin^2\alpha + \frac{g(\rho\beta)_{hnf}(T - T_\infty)}{\rho_{hnf}}\sin\Omega \tag{2}$$

Energy equation:

$$(\rho C_p)_{hnf}(uT_x + vT_r) = k_{hnf}\left(\frac{1}{r}\right)(rT_r)_r \tag{3}$$

With the boundary conditions[6],

$$\left.\begin{array}{c} u = U_w + \Gamma_1\left(\frac{\mu_{hnf}}{\rho_{hn}}\right)\frac{\partial u}{\partial r}, v = 0, T = T_w + \Gamma_2\frac{\partial T}{\partial r}atr = R(x) \\ u \to u_\infty, T \to T_\infty\ as\ r \to \infty \end{array}\right\} \tag{4}$$

The hybrid nanofluid is strategized different volumetric solid fractions $(\phi_1, \phi_2)$ such as $Al_2O_3 - (0.5\%)$ and $Fe_3O_4 - (1.5\%)$.

The hybrid nanofluid properties are considered by Sajja et al.[13].

$$\rho_{hnf} = \{(1-\phi_2)[(1-\phi_1)\rho_f + \phi_1\rho_{s_1}]\} + \phi_2\rho_{s_2} \tag{5}$$

$$\mu_{hnf} = \frac{\mu_f}{(1-\phi_1)^{2.5}(1-\phi_2)^{2.5}} \tag{6}$$

$$k_{hnf} = \frac{k_{s_2} + 2k_{nf} - 2\phi_2(k_{nf} - k_{s_2})}{k_{s_2} + 2k_{nf} + \phi_2(k_{nf} - k_{s_2})} \times k_{nf} \tag{7}$$

$$k_{nf} = \frac{k_{s_1} + 2k_f - 2\phi_1(k_f - k_{s_1})}{k_{s_1} + 2k_f + \phi_1(k_f - k_{s_1})} \times k_f \tag{8}$$

$$(\rho C_p)_{hnf} = \{(1-\phi_2)[(1-\phi_1)(\rho C_p)_f + \phi_1(\rho C_p)_{s_1}]\} + \phi_2(\rho C_p)_{s_2} \tag{9}$$

$$(\rho\beta)_{hnf} = \{(1-\phi_2)[(1-\phi_1)(\rho\beta)_f + \phi_1(\rho\beta)_{s_1}]\} + \phi_2(\rho\beta)_{s_2} \tag{10}$$

Along with variables such as[13],

$$\left.\begin{aligned} \varepsilon = \frac{Ur^2}{\nu x}, \psi = \nu x f(\varepsilon), u = \frac{1}{r}\left(\frac{\partial\psi}{\partial r}\right) \\ v = -\frac{1}{r}\left(\frac{\partial\psi}{\partial x}\right), T = T_\infty + (T_w - T_\infty)\theta(d) \end{aligned}\right\} \tag{11}$$

we can get $R(x) = \left(\frac{\nu dx}{U}\right)^{\frac{1}{2}}$ where $U = U_w + U_\infty \neq 0$ is the governing equations is satisfied by reinforced acceleration. and transforms (Equations (2) and (3)) as:

$$\frac{2}{E_1E_2}(\varepsilon F''' + F'') - \frac{1}{2E_2}MF'sin^2\alpha + \lambda E_5(sin\Omega)\theta = 0 \tag{12}$$

$$\frac{2E_3E_{31}}{E_4}\frac{1}{Pr}(\varepsilon\theta'' + \theta') + F\theta' = 0 \tag{13}$$

and changes the circumstances in Equation (4) as,

$$\left.\begin{aligned} F'(d) = \frac{\delta}{2} + \frac{2\gamma_1\sqrt{d}}{E_1E_2}, F(d) = d\left(\frac{\delta}{2} + \frac{2\gamma_1\sqrt{d}}{E_1E_2}\right), \theta(d) = 1 + \gamma_2\theta'(\varepsilon) \\ F'(\infty) \to \frac{1-\delta}{2}, \theta(\infty) \to 0 \end{aligned}\right\} \tag{14}$$

The hybrid nanofluid properties are considered by Sajja et al.[13].

$$E_1 = (1-\phi_1)^{2.5}(1-\phi_2)^{2.5} \tag{15}$$

$$E_2 = \left\{(1-\phi_2)\left[(1-\phi_1) + \phi_1\frac{\rho_{s1}}{\rho_f}\right]\right\} + \phi_2\frac{\rho_{s2}}{\rho_f} \tag{16}$$

$$E_{31} = \frac{k_{s1} + 2k_f - 2\phi_1(k_f - k_{s1})}{k_{s1} + 2k_f + \phi_1(k_f - k_{s1})} \tag{17}$$

$$E_3 = \frac{k_{s2} + 2E_{31}k_f - 2\phi_2(E_{31}k_f - k_{s2})}{k_{s2} + 2E_{31}k_f + \phi_2(E_{31}k_f - k_{s2})} \tag{18}$$

$$E_4 = (1-\phi_2)\left[(1-\phi_1) + \phi_1\frac{(\rho C_p)_{s1}}{(\rho C_p)_f}\right] + \phi_2\frac{(\rho C_p)_{s1}}{(\rho C_p)_f} \tag{19}$$

$$E_5 = (1-\phi_2)\left[(1-\phi_1) + \phi_1\frac{(\rho\beta)_{s1}}{(\rho\beta)_f}\right] + \phi_2\frac{(\rho\beta)_{s2}}{(\rho\beta)_f} \tag{20}$$

$$Gr_x = \frac{g\beta_f(T_w - T_\infty)L^3}{\nu^2}, Re_x = \frac{UL}{\nu}, M = \frac{\sigma B_0^2}{\rho U}, \delta = \frac{U_w}{U} = \frac{constant\ velocity}{composite\ velocity} \tag{21}$$

$$\lambda = \frac{Gr_x}{Re_x^2} = \frac{g\beta_f(T_w - T_\infty)L^3}{U^2}, Pr = \frac{\mu c_p}{k} \tag{22}$$

### Nusselt number and skin friction

Another important external of the contemporary examination is the Nusselt number, Skin friction which is prearranged by,

$$N_{ux} = \frac{xq_w}{k_f\left((T_w - T_\infty)\right)}\Big|_{r=R(x)} \tag{23}$$

$$C_{fx} = \frac{\tau_w}{\frac{1}{2}\rho U^2}\Big|_{r=R(x)} \tag{24}$$

where $q_w = -k_{hnf}\frac{\partial T}{\partial r}(wall\ heat\ flux),\ \tau_w = \mu_{hnf}\frac{\partial u}{\partial r}\ (wall\ shear\ stress)$.

The following terms from Equations (19) and (20) are described in non-dimensional form

$$(Re_x)^{-\frac{1}{2}}N_{ux} = -E_3E_{31}2\sqrt{d}\theta'(d) \tag{25}$$

$$(Re_x)^{-\frac{1}{2}}C_{fx} = \frac{8F''(\varepsilon)\sqrt{d}}{E_1} \tag{26}$$

where $Re_x = \frac{UL}{\nu}(Reynolds\ number)$.

## 3. Entropy analysis

The countenance for the entropy analysis is specified below[35]

$$S_{gen}^{'''} = \frac{k}{T_\infty^2}((T_r)^2) + \frac{\mu}{T_\infty}((u_r)^2) + \frac{\sigma B_0^2}{T_\infty}u^2 \tag{27}$$

where the primary term displays the entropy analysis proportion due to heat transmission $S_h^{'''}$, the next term confirms the entropy analysis proportion due to fluid resistance $S_f^{'''}$, the third tenure illustrates the entropy analysis proportion owing to the magnetic field $S_m^{'''}$.

$$S_{gen}^{'''} = S_h^{'''} + S_f^{'''} + S_m^{'''} \tag{28}$$

The proportion of total entropy analysis that can remain engraved in a dimensionless process is

$$N_s = \frac{S_{gen}^{'''}}{\left(\frac{4k_f}{x^2}\right)\Omega_T} = \varepsilon Re_x\Omega_T\theta'^2 + 4\varepsilon Re_x BrF''^2 + MRe_x BrF'^2 \tag{29}$$

where $Br = \frac{\mu U^2}{k_f(T_w - T_\infty)}$ represents the Brinkman number.

### Bejan analysis

Regarding the entropy analysis examination of convective heat transmission issues, Bejan stated the irreversibility distribution proportion as follows:

$$\Phi = \frac{S_{prod,frc}^{'''}}{S_{prod\ ,\Delta T}^{'''}} \tag{30}$$

It is imperative to note that the fluid resistance ($N_{sf}$) irreversibility plays a major role when $\Phi > 1$. Therefore, the heat transmission irreversibility ($N_{sh}$) is fundamental. When $\Phi = 1$, the perfections related to heat transference ($N_{sh}$) and fluid resistance ($N_{sf}$) are the equivalent.

Equation $\Phi$ could very well establish.

$$\Phi = \frac{4BrF''^2 + \frac{Br}{\Omega T\eta} MF'^2}{\theta'^2} \tag{31}$$

The impermissibility ratio, or Bejan multitude, is

$$Be = \frac{S'''_{prod,\Delta T}}{S'''_{prod}} = \frac{\frac{k}{T_\infty^2}((T_r)^2)}{\frac{k}{T_\infty^2}((T_r)^2) + \frac{\mu}{T_\infty}((u_r)^2)} \tag{32}$$

As a direct consequence of the method developed, it begins to develop in and out of

$$Be = \frac{\theta'^2}{\theta'^2 + 4BrF''^2 + \frac{Br}{\Omega T\eta} MF'^2} \tag{33}$$

$Be = 1$ symbolizes the boundary at which irreversibility is entirely owed to heat transmission,
$Be = 0$ is the boundary at which the irreversibility is due to fluid resistance only.
$Be >> 1/2$ when irreversibility outstanding to heat transmission takes antecedence.
$Be << 1/2$ demonstrates that irreversibility due to fluid resistance is foremost.

## 4. Physical explanation

Analyzing this research needs to resolve the governing equivalences for mass, velocity, and thermal conservation. These equations are typically solved using numerical techniques such as BVP4C. The governing equations for this problem can be expressed in non-dimensional form using suitable dimensionless variables such as Reynolds variable, Prandtl quantity, and inclined magnetic. **Figures 2–16** depict the appearances and structures of various pertinent variables appearing in the problematic profiles of hybrid nanofluid momentum, thermal, entropy, and the Bejan profile. **Table 1** demonstrates the importance of magnetic and nonmagnetic nanoparticle thermophysical properties, as well as hybrid nanofluid thermal properties. **Table 2** displays heat transfer rate and surface drag force values. **Table 3** and **Figures 17** and **18** compare our results to available outcomes in order to validate our problem with other research and discover its remarkable similarity. The transmuted nonlinear differential Equations (1)–(3), moreover, the boundary restriction (Equations (13) and (14)), are numerically resolved using the BVP4C solver. The values that appear in the problem through computation are fixed as $\phi_1 = 0.005$, $\phi_2 = 0.015$, $d = 0.5$, $Pr = 29.45$, $M = 3$, $\delta = 1, v_1 = t_1 = 1.5$. The detailed numerical solution is below,

$$y_1 = f \; and \; y_4 = \theta$$

$$y_1' = y_2$$

$$y_2' = y_3$$

$$y_3' = -\frac{1}{\varepsilon}\left[y_3 + \frac{E_1E_2}{2}\left(y_1y_3 - \frac{1}{2E_2} \times y_2 \times X + \lambda E_5(\sin\Omega)y_4\right)\right]$$

$$y_4' = y_5$$

$$y_5' = \frac{1}{\varepsilon}\left[-y_5 - \frac{E_4}{2E_3E_{31}} \times Pr \times y_1y_5\right]$$

$$y_2(a) = \frac{\delta}{2} + \frac{\nu_{1\sqrt{d}}}{2} \times \frac{1}{E_1 E_2}$$

$$y_1(a) = d * \left[\frac{\delta}{2} + \frac{\nu_{1\sqrt{d}}}{2} * \frac{1}{E_1 E_2}\right]$$

$$y_4(a) = 1 + t_1 * y_5$$

$$y_2(b) = \frac{1-\delta}{2}$$

$$y_4(b) = 0$$

**Table 2.** Disparity of $d, M, \phi_1, \phi_2, Pr, \alpha, \lambda$ on $Nu_x$ and $Cf_x$.

| $Nu_x$ and $Cf_x$ | | | | | | | | |
|---|---|---|---|---|---|---|---|---|
| **d** | **M** | $\phi_1$ | $\phi_2$ | $Pr$ | $\alpha$ | $\lambda$ | $Nu_x$ | $Cf_x$ |
| 1 | 3 | 0.005 | 0.015 | 29.45 | $45^0$ | 0.5 | 1.3892 | −92.2282 |
| 2 | | | | | | | 1.3717 | −51.7194 |
| 3 | | | | | | | 1.3551 | −38.5092 |
| 1 | 1 | 0.005 | 0.015 | 29.45 | $45^0$ | 0.5 | 1.3892 | −89.5042 |
| | 2 | | | | | | 1.3892 | −90.8821 |
| | 3 | | | | | | 1.3892 | −92.2282 |
| 1 | 3 | 0.005 | 0.015 | 29.45 | $45^0$ | 0.5 | 1.3892 | −92.2282 |
| | | 0.010 | | | | | 1.4091 | −93.3588 |
| | | 0.015 | | | | | 1.4292 | −94.5255 |
| 1 | 3 | 0.005 | 0.015 | 29.45 | $45^0$ | 0.5 | 1.3892 | −92.2282 |
| | | | 0.020 | | | | 1.4073 | −92.9950 |
| | | | 0.025 | | | | 1.4255 | −93.8023 |
| 1 | 3 | 0.005 | 0.015 | 1 | $45^0$ | 0.5 | 1.1444 | −92.1319 |
| | | | | 2 | | | 1.2317 | −92.1868 |
| | | | | 3 | | | 1.2747 | −92.2051 |
| 1 | 3 | 0.005 | 0.015 | 29.45 | $0^0$ | 0.5 | 1.3892 | −88.0924 |
| | | | | | $45^0$ | | 1.3892 | −92.2282 |
| | | | | | $90^0$ | | 1.3892 | −92.6414 |
| 1 | 3 | 0.005 | 0.015 | 29.45 | $45^0$ | 0.5 | 1.3892 | −92.2282 |
| | | | | | | 1.5 | 1.3892 | −92.2273 |
| | | | | | | 2.5 | 1.3892 | −92.2264 |

**Table 3.** Assertion of present rankings when volumetric solid fractions $(\phi_1, \phi_2)$ and the velocity ratio parameter $\delta$ are zero.

| | **Reference 13 (Sajja)** | | **Present outcomes** | |
|---|---|---|---|---|
| $\varepsilon$ | $F''(\varepsilon)$ | $-\theta'(\varepsilon)$ | $F''(\varepsilon)$ | $-\theta'(\varepsilon)$ |
| 0.1 | 1.289074 | 2.441675 | 1.287564 | 2.438536 |
| 0.01 | 8.492173 | 16.306544 | 8.490543 | 16.282928 |
| 0.001 | 62.161171 | 120.55034 | 62.148128 | 120.254769 |

# 5. Review and discussion of the results

**Figure 1** depicts the items placed in the conundrum. In regard to physical behaviour and attitude are explanations in the figures. **Figures 2–16** have been drawn for EG-Water (50:50) + $Al_2O_3$ + $Fe_3O_4$, to demonstrate the impression of numerous parameters on acceleration, entropy generation, and Bejan number.

## 5.1. Velocity and thermal profile

**Figure 2** explains the increase in the magnetic parameter ($M = 1, 2, 3$) strengthens the opposing magnetic force, while the increase in the inclination angle ($\Omega = 0^o, 45^o, 90^o$) magnifies the gravitational force component acting parallel to the surface. Both of these factors contribute to a decline in the velocity profile of the inclined needle.

Velocity profile:

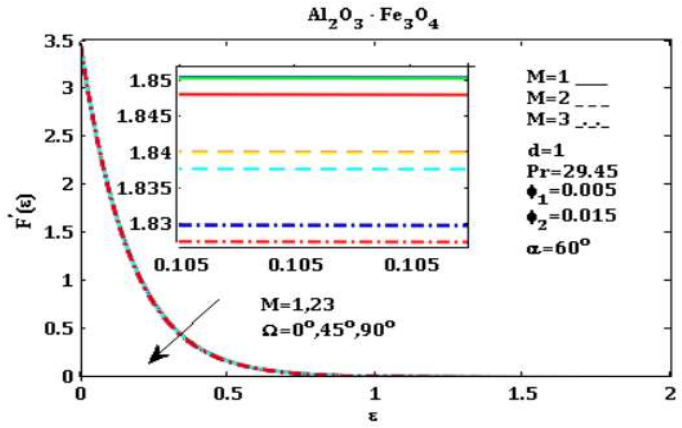


**Figure 2.** The impacts of $M = 1, 2, 3$ on $F'(\varepsilon)$.

When both the needle size ($d = 0.5, 1, 1.5$) and angle ($\Omega = 0^o, 45^o, 90^o$) increase simultaneously, their combined effect enhances the fluid flow even more. The larger needle diameter allows for a greater fluid volume, while the steeper angle generates a higher pressure drop. This combination results in a more pronounced upsurge in the velocity profile, as explained in **Figure 3**.

Velocity profile:

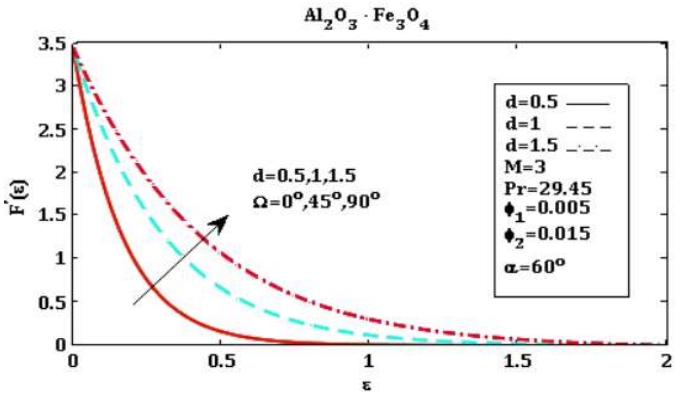


**Figure 3.** The impacts of $d = 0.5, 1, 1.5$ on $F'(\varepsilon)$.

**Figure 4** explains that when the velocity, temperature slip parameter ($v_1 = t_1 = 1.5, 2.5, 3.5$), and angle ($\Omega = 0^o, 45^o, 90^o$) of an inclined needle are increased, the velocity profile tends to become more

uniform and less parabolic. The increased velocity promotes turbulence, the higher temperature slip parameter introduces thermal effects, and the steeper angle amplifies the influence of gravity. These factors combine to produce a higher velocity profile along the surface of the needle.

Velocity profile:

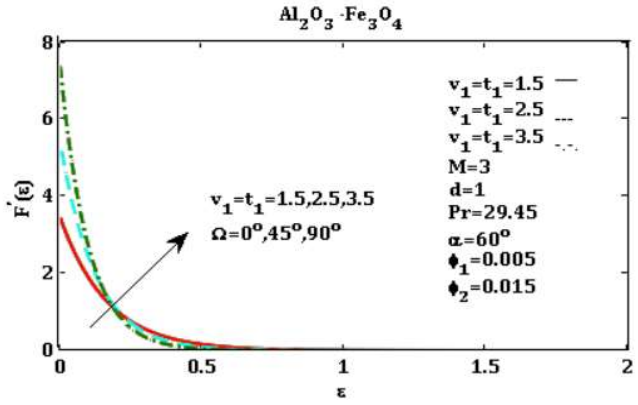


**Figure 4.** The impacts of $v_1 = t_1 = 1.5, 2.5, 3.5$ on $F'(\epsilon)$.

As shown in **Figure 5**, when both the velocity ratio parameter ($\delta = 1, 2, 3$) and the angle ($\Omega = 0^o, 45^o, 90^o$) increase, the fluid experiences an increased velocity due to a combination of factors. The higher velocity ratio parameter indicates a faster flow rate, while the increased angle leads to a more pronounced directional component of the fluid velocity. As a result, the overall momentum profile of the fluid in the inclined needle increases.

Velocity profile:

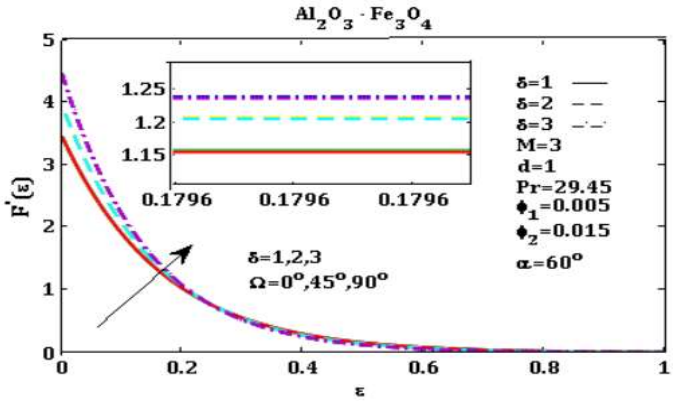


**Figure 5.** The impacts of $\delta = 1, 2, 3$ on $F'(\varepsilon)$.

A mixed convection parameter is a dimensionless number that characterizes a system's relative importance of forced and natural convection. When both the mixed convection parameter ($\lambda = 0.5, 1.5, 2.5$) and the angle of inclination ($\Omega = 0^o, 45^o, 90^o$) increase simultaneously, the mutual consequence of enhanced forced convection and increased natural convection results in an even greater velocity profile in the inclined needle. The fluid is influenced by both the external source (forced convection) and the buoyancy forces (natural convection), leading to an intensified flow pattern with higher velocities, as appeared in **Figure 6**.

Velocity profile:

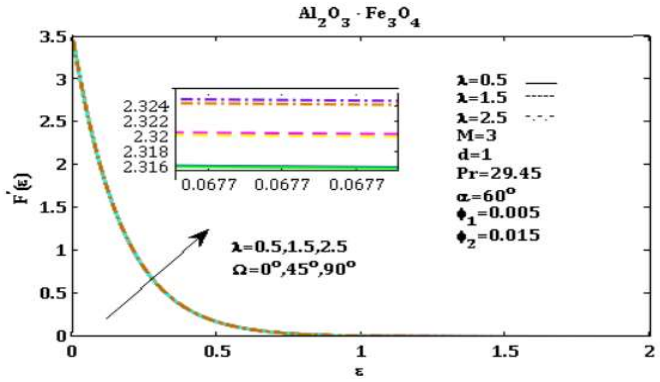


**Figure 6.** The impacts of $\alpha = 0^o, 45^o, 90^o$ on $F'(\varepsilon)$.

**Figure 7** explains that when both the magnetic parameter ($M = 1, 2, 3$) and the inclination angle ($\Omega = 0^o, 45^o, 90^o$) increase simultaneously, their combined effects result in a more pronounced enhancement of heat transfer. The stronger magnetic field induces more vigorous fluid motion, while the larger inclination angle modifies the buoyancy-driven flow patterns. These changes collectively lead to increased heat transfer from the needle, resulting in an increase in the temperature profile.

Thermal profile:

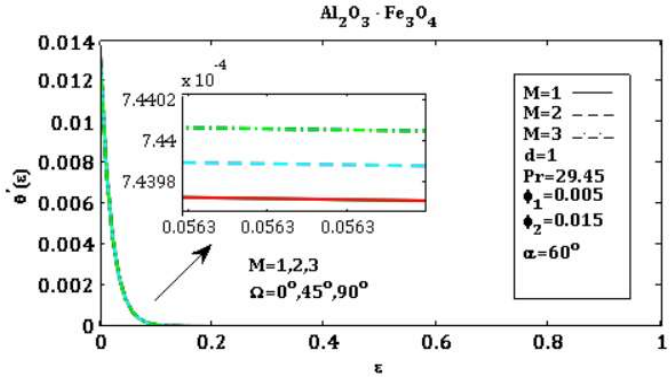


**Figure 7.** The impact of $M = 1, 2, 3$ on $\theta'(\varepsilon)$.

When both the needle size ($d = 0.5, 1, 1.5$) and angle ($\Omega = 0^o, 45^o, 90^o$) increase, the combined effect of increased surface area (due to larger needle size) and enhanced convection (due to higher needle angle) can outweigh the reduction in the surface area caused by the inclination. This results in an overall intensification in the temperature profile of the inclined needle, as exposed in **Figure 8**.

Thermal profile:

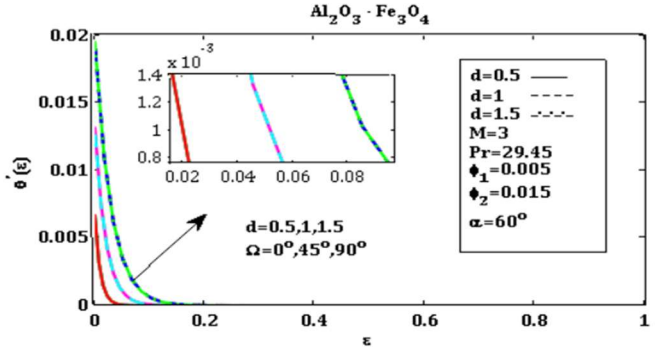


**Figure 8.** The impact of $d = 0.5, 1, 1.5$ on $\theta'(\varepsilon)$.

**Figure 9** explains that when the velocity, temperature slip parameter ($v_1 = t_1 = 1.5, 2.5, 3.5$), and angle ($\Omega = 0^o, 45^o, 90^o$) increase in an inclined needle, the temperature profile tends to decrease. This is primarily due to enhanced convective heat transfer resulting from higher fluid velocity, a larger temperature difference at the interface (temperature slip parameter), and increased fluid turbulence caused by the inclination angle.

Thermal profile:

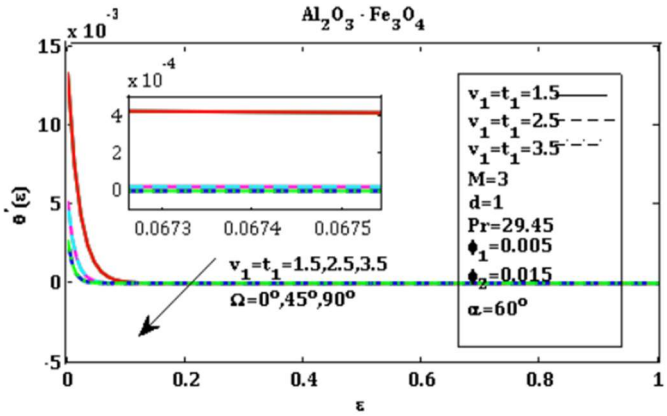


**Figure 9.** The impact of $v_1 = t_1 = 1.5, 2.5, 3.5$ on $\theta'(\varepsilon)$.

When both the velocity ratio ($\delta = 1, 2, 3$) parameter and the angle ($\Omega = 0^o, 45^o, 90^o$) of inclination increase, the combined effect is a significant enhancement in fluid mixing and heat transfer. The increased velocity ratio increases turbulence and shear stresses, promoting better mixing. The increased angle of inclination strengthens the gravity-driven flow, further enhancing the mixing. The enhanced mixing and heat transfer result in a more efficient transmission of thermal energy from the fluid to the needle walls. Consequently, the temperature profile of the fluid decreases explained in **Figure 10**.

Thermal profile:

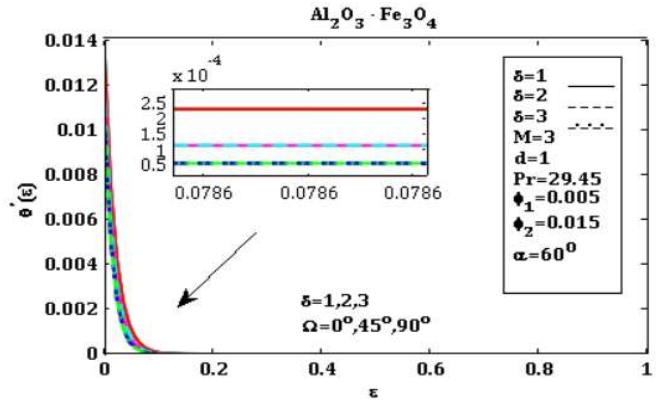


**Figure 10.** The impacts of $\delta = 1, 2, 3$ on $\theta'(\varepsilon)$.

## 5.2. Entropy and Bejan profile

The relationship between aluminium oxide and magnetic parameters would largely depend on the introduction of magnetic impurities or the formation of composite materials. If aluminium oxide is doped with magnetic elements or combined with magnetic materials, then its magnetic properties can be influenced by an inclined needle. As the magnetic parameter (field strength or magnetic moment)

increases, the alignment of the needle with the field may become more pronounced. This alignment can affect the entropy distribution along the needle, as shown in **Figure 11**.

Entropy and Bejan profile:

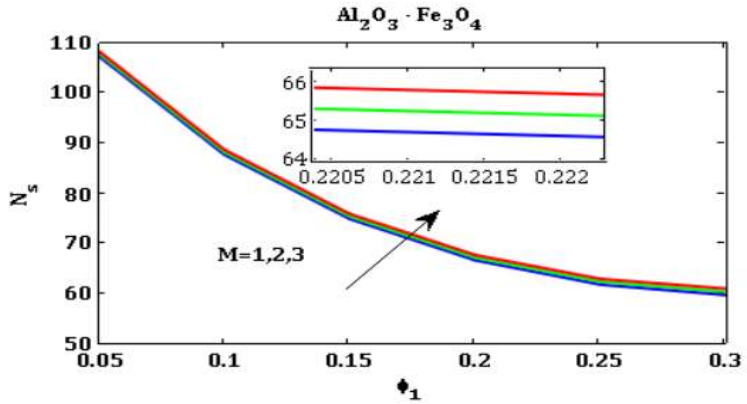


**Figure 11.** Relationship between $M$ and $\phi_1$ on entropy profile.

The relationship between (*Br*) and (*Re*) determines the behavior of the fluid flow. As the Brinkman number increases, the flow becomes more influenced by viscous forces, leading to an increase in the entropy profile. This is because higher viscous forces result in more energy dissipation and heat generation within the flow. Consequently, entropy, which is a measure of the disorder or randomness of a system, tends to increase, as shown in **Figure 12**.

Entropy and Bejan profile:

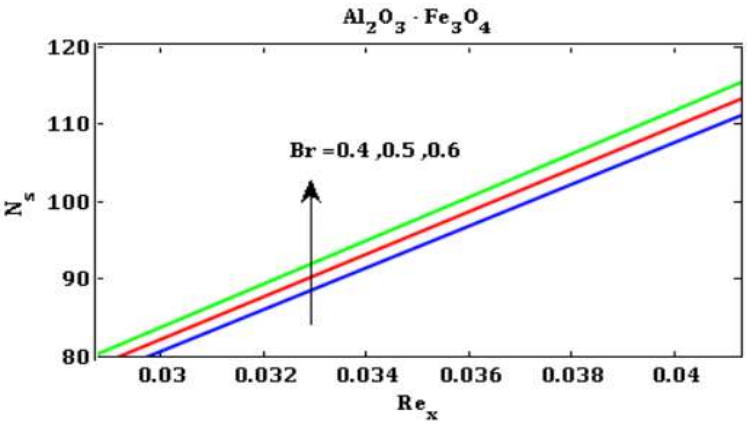


**Figure 12.** Relationship between $Br$ and $Re_x$ on entropy profile.

**Figure 13** explained that the relationship between the (*Br*) and (*M*) determines the behavior of the fluid flow. The Brinkman number represents the proportion of viscous forces to inertial forces. This implies that the fluid flow is more influenced by the viscosity of the fluid. When the magnetic parameter increases, it signifies a stronger influence of the magnetic field on the fluid flow. In the presence of a magnetic field, the fluid may experience additional forces and interactions, such as magnetic induction and Lorentz forces. These forces can alter the flow behaviour and have an impact on the entropy profile.

Entropy and Bejan profile:

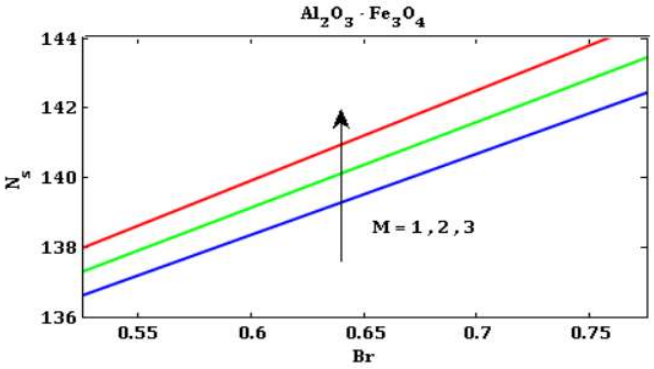


**Figure 13.** Relationship between $Br$ and $M$ on entropy profile.

The relationship between a magnetic field and a nanoparticle of $Al_2O_3$, specifically in the context of a horizontal needle, as the magnetic field $M = (1, 2, 3)$, increases, the Bejan number decreases in the case of a horizontal needle with a nanoparticle of $Al_2O_3$. Since the Bejan number is inversely proportional to the convective heat transfer, an intensification in convective heat transfer caused by the altered flow pattern will result in a decrease in the Bejan number, as shown in **Figure 14**.

Entropy and Bejan profile:

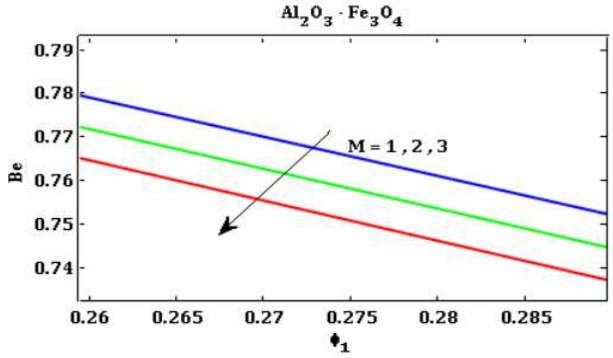


**Figure 14.** Relationship between $M$ and $\phi_1$ on bejan profile.

**Figure 15** explained the relationship between the Brinkman number and the Reynolds number in the context of flow around a horizontal needle. As the Brinkman number ($Br = 0.1, 0.2, 0.3$) increases, the viscous dissipation becomes more significant, leading to a decrease in convective heat transfer and a decrease in the Bejan number.

Entropy and Bejan profile:

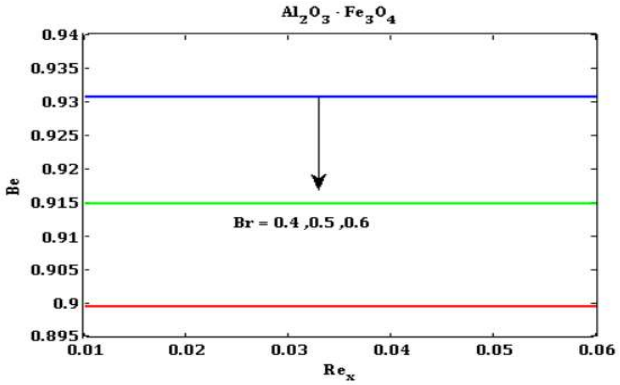


**Figure 15.** Relationship between $Br$ and $Re_x$ on bejan profile.

The relationship between the Brinkman number and the magnetic field is that when the magnetic field $M = (1, 2, 3)$ increases, the convective heat transfer tends to decrease, while the conductive heat transfer may remain relatively unchanged. Consequently, the ratio of heat conduction to convective heat transfer, represented by the Bejan number decreases, as explained in **Figure 16**.

Entropy and Bejan profile:

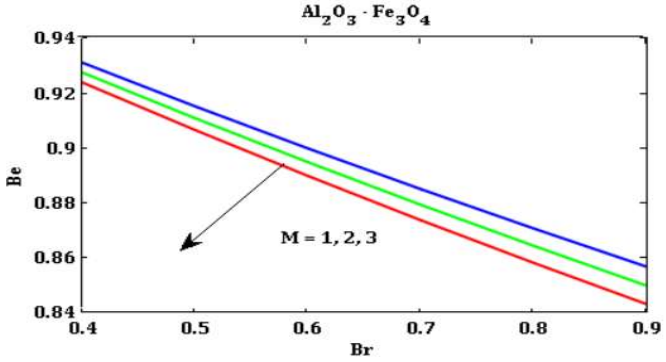


**Figure 16.** Relationship between $Br$ and $M$ on bejan profile.

**Table 2** examined the heat transfer rate and surface drag force for various parameters. The values that appear in the problem through computation are fixed as $\phi_1 = 0.005$, $\phi_2 = 0.015$, $d = 1$, $Pr = 29.45$, $M = 3$, $\delta = 1$, $v_1 = t_1 = 1.5$, $\alpha = 45^o$, $\lambda = 0.5$, $\Omega = 45^o$. According to Sajja et al.[13], the assessment of $f''(\varepsilon)$ and $-\theta'(\varepsilon)$ is revealed in **Table 3** when $\phi_1 = \phi_2 = \delta = 0$, and also it's explained graphically in **Figures 17** and **18**.

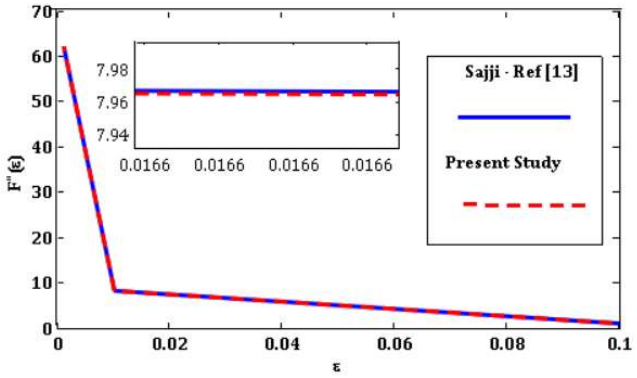


**Figure 17.** Comparison of $F''(\varepsilon)$[13].

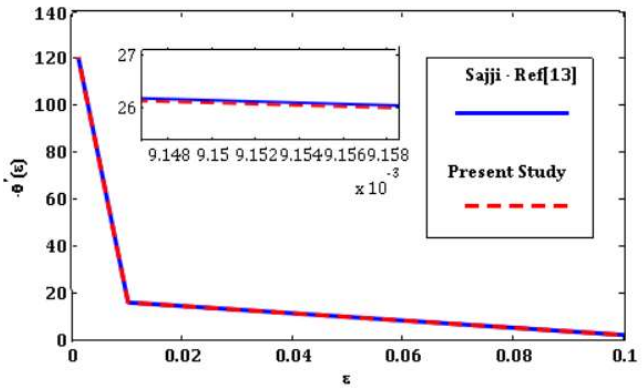


**Figure 18.** Comparison of $-\theta'(\varepsilon)$[13].

## 6. Conclusion

Analyzed in this paper, the main thing entropy generation in a magnetohydrodynamic (MHD) slip flow with a hybrid nanofluid over an inclined needle involves investigating the effects of fluid flow, magnetic field, and nanoparticle additives on the thermodynamic performance of the system. This analysis can provide valuable insights into the efficiency and energy losses in the flow and is essential for optimizing the design and operation of such systems. The effects of an inclined Lorentz force and entropy generation on the flow of ferrous and aluminum oxide nanoparticles in a hybrid nanoliquid with water and ethylene glycol (50:50) as base fluids have been analysed numerically.

- The presence of nanoparticles in the base fluid can significantly enhance heat transfer characteristics, leading to improved thermal performance compared to conventional fluids. The heat transfer rate can be influenced by various factors such as nanoparticle volume fraction, size, shape, and type.
- Effects of magnetic field: the presence of a magnetic field can alter the flow and heat transfer behavior in MHD slip flow. Magnetic fields can induce fluid motion, alter nanoparticle distribution, and affect the heat transfer rate.
- The angle of inclination can influence the flow pattern, boundary layer formation, and consequently, the overall heat transfer and entropy generation.
- The entropy generation rate is given by the product of the local irreversibility and the volume element. The irreversibility term can be calculated based on the flow variables and their gradients.
- The velocity ratio has a higher bearing, and the thermal profile has decreased.
- Entropy generation analysis helps quantify the irreversibilities within the system. It provides insights into the energy losses and efficiency of the process.
- The entropy rate increases with increasing the values of Brinkman, Reynolds, and magnetic field criteria.

Understanding MHD and slip flow phenomena is crucial for engineering applications like aerospace, energy, and biomedical fields. Entropy generation analysis optimizes systems for efficiency, reduced energy losses, and cost savings, while energy-related research contributes to sustainable practices and reduced environmental impact. Researchers can optimize MHD systems by considering practical constraints like material properties, manufacturing limitations, and cost, leading to viable engineering solutions. This approach could be applied in nanofluids, advanced materials, and biomedical devices.

## Author contributions

Conceptualization, AKAH and SP; methodology, AKAH; software, BG; validation, AKAH, BG and PR; formal analysis, AKAH; investigation, AKAH; resources, GRR; data curation, GRR; writing—original draft preparation, SP; writing—review and editing, SP; visualization, BG; supervision, AKAH; project administration, AKAH; funding acquisition, BG. All authors have read and agreed to the published version of the manuscript.

## Conflict of interest

The authors declare no conflict of interest.

# Nomenclature

| | |
|---|---|
| $B$ | Magnetic field intensity, $kgs^{-2}a^{-1}$ |
| $C_f$ | Skin friction coefficient |
| $C_p$ | Specific heat, $jkg^{-1}k^{-1}$ |
| $K$ | Thermal conductivity, $wm^{-1}k^{-1}$ |
| $M$ | Magnetic parameter |
| $Nu_x$ | Local Nusselt number |
| $Pr$ | Prandtl number |
| $q_w$ | Surface heat flux, $wm^{-2}$ |
| $Re$ | Local reynolds number |
| $Gr_x$ | Grashof number |
| $R(x)$ | Equivalence of the surface of a thin needle |
| $F$ | Dimensionless fluid velocity |
| $T$ | Temperature of fluid |
| $T_w$ | Ambient thermal |
| $T_\infty$ | Surface thermal |
| $U$ | Reference velocity, $ms^{-1}$ |
| $U_w$ | Constant velocity |
| $U_\infty$ | Free stream momentum |
| $u$ | Momentum factor in the x way |
| $x, r$ | Cylindrical directs |
| Greek letters | |
| $\alpha$ | Angle |
| $\beta$ | Thermal expansion coefficient |
| $\varepsilon$ | The magnitude of the needle ($\varepsilon$ = d) |
| $\phi_1, \phi_2$ | Nanoparticles of volume fraction |
| $\mu$ | Dynamic viscosity, $kgm^{-1}s^{-1}$ |
| $\upsilon$ | Kinematic viscosity, $m^2s^{-1}$ |
| $\sigma$ | Electrical conductivity, $sm^{-1}$ |
| $\rho$ | Density, $kgm^{-3}$ |
| $\theta$ | Dimensionless fluid temperature |
| $\lambda$ | Mixed convection parameter |
| $\delta$ | Velocity ratio parameter |
| $\psi$ | Dimensionless stream function |
| $\tau_w$ | Wall shear stress, $nm^{-2}$ |
| $\Gamma_1$ | Velocity slip factor |
| $\Gamma_2$ | Thermal slip factor |
| $\gamma_1$ | Velocity slip coefficient |
| $\gamma_2$ | Thermal slip coefficient |
| Subscripts | |
| *Hnf* | Hybrid nanofluid |
| *Nf* | Nanofluid |

| | |
|---|---|
| *F* | Fluid |
| *S* | Solid |

## References


1. Balmforth NJ, Craster RV, Rust AC, Sassi R. Viscoplastic flow over an inclined surface. *Journal of Non-Newtonian Fluid Mechanics* 2007; 142(1–3): 219–243. doi: 10.1016/j.jnnfm.2006.07.013
2. Wong J, Lindstrom M, Bertozzi AL. Fast equilibration dynamics of viscous particle-laden flow in an inclined channel. *Journal of Fluid Mechanics* 2019; 879: 28–53. doi: 10.1017/jfm.2019.685
3. Bano N, Singh BB. An integral treatment for coupled heat and mass transfer by natural convection from a radiating vertical thin needle in a porous medium. *International Communications in Heat and Mass Transfer* 2017; 84: 41–48. doi: 10.1016/j.icheatmasstransfer.2017.03.007
4. Choi SUS, Eastman JA. Enhancing thermal conductivity of fluids with nanoparticles. In: Proceedings of 1995 International Mechanical Engineering Congress and Exhibition; 12–17 November 1995; San Francisco, US.
5. Iqbal Z, Yashodha S, Abdul Hakeem AK, et al. Energy transport analysis in natural convective flow of water: Ethylene glycol (50:50)-based nanofluid around a spinning down-pointing vertical cone. *Frontiers in Materials* 2022; 9: 1037201. doi: 10.3389/fmats.2022.1037201
6. Ganesh NV, Al-Mdallal QM, Reena K, Aman S. Blasius and Sakiadis slip flow of $H_2O$–$C_2H_6O_2$ (50:50) based nanoliquid with different geometry of boehmite alumina nanoparticles. *Case Studies in Thermal Engineering* 2019; 16: 100546. doi: 10.1016/j.csite.2019.100546
7. Chamkha AJ, Rashad AM, Mansour MA, et al. Effects of heat sink and source and entropy generation on MHD mixed convection of a Cu-water nanofluid in a lid-driven square porous enclosure with partial slip. *Physics of Fluids* 2017; 29(5): 052001. doi: 10.1063/1.4981911
8. Khan WA. Significance of magnetized Williamson nanofluid flow for ferromagnetic nanoparticles. *Waves in Random and Complex Media* 2023. doi: 10.1080/17455030.2023.2207390
9. Khan WA. Impact of time-dependent heat and mass transfer phenomenon for magnetized Sutterby nanofluid flow. *Waves in Random and Complex Media* 2022. doi: 10.1080/17455030.2022.2140857
10. Irfan M, Khan WA, Pasha AA, et al. Significance of non-Fourier heat flux on ferromagnetic Powell-Eyring fluid subject to cubic autocatalysis kind of chemical reaction. *International Communications in Heat and Mass Transfer* 2022; 138: 106374. doi: 10.1016/j.icheatmasstransfer.2022.106374
11. Anjum N, Khan WA, Hobiny A, et al. Numerical analysis for thermal performance of modified Eyring Powell nanofluid flow subject to activation energy and bioconvection dynamic. *Case Studies in Thermal Engineering* 2022; 39: 102427. doi: 10.1016/j.csite.2022.102427
12. Tabrez M, Khan WA. Exploring physical aspects of viscous dissipation and magnetic dipole for ferromagnetic polymer nanofluid flow. *Waves in Random and Complex Media* 2022. doi: 10.1080/17455030.2022.2135794
13. Sajja VS, Gadamsetty R, Muthu P, et al. Significance of Lorentz force and viscous dissipation on the dynamics of propylene glycol: Water subject to Joule heating conveying paraffin wax and sand nanoparticles over an object with a variable thickness. *Arabian Journal for Science and Engineering* 2022; 47: 15505–15518. doi: 10.1007/s13369-022-06658-z
14. Sen SSS, Das M, Nayak MK, Makinde OD. Natural convection and heat transfer of micropolar hybrid nanofluid over horizontal, inclined and vertical thin needle with power-law varying boundary heating conditions. *Physica Scripta* 2023; 98: 015206. doi: 10.1088/1402-4896/aca3d7
15. Waqas M, Khan WA, Ali Pasha A, et al. Dynamics of bioconvective Casson nanoliquid from a moving surface capturing gyrotactic microorganisms, magnetohydrodynamics and stratifications. *Thermal Science and Engineering Progress* 2022; 36: 101492. doi: 10.1016/j.tsep.2022.101492
16. Hussian Z, Khan WA. Impact of thermal-solutal stratifications and activation energy aspects on time-dependent polymer nanoliquid. *Waves in Random and Complex Media* 2022. doi: 10.1080/17455030.2022.2128229
17. Salahuddin T, Akram A, Awais M, Khan M. A hybrid nanofluid analysis near a parabolic stretched surface. *Journal of the Indian Chemical Society* 2022; 99(8): 100558. doi: 10.1016/j.jics.2022.100558
18. Indhumathi N, Ganga B, Charles S, Abdul Hakeem AK. Magnetohydrodynamics boundary layer flow past a wedge of Casson CuO-$TiO_2$/EG embedded in non-Darcian porous media: Viscous dissipation effects. *Journal of Nanofluids* 2022; 11(6): 906–914. doi: 10.1166/jon.2022.1888
19. Salahuddin T, Akram A, Khan M, Altanji M. A curvilinear approach for solving the hybrid nanofluid model. *International Communications in Heat and Mass Transfer* 2022; 137: 106179. doi: 10.1016/j.icheatmasstransfer.2022.106179

20. Mahdy A, El-Zahar ER, Rashad AM, et al. The magneto-natural convection flow of a micropolar hybrid nanofluid over a vertical plate saturated in a porous medium. *Fluids* 2021; 6(6): 202. doi: 10.3390/fluids6060202
21. El-Zahar ER, Mahdy AEN, Rashad AM, et al. Unsteady MHD mixed convection flow of non-Newtonian Casson hybrid nanofluid in the stagnation zone of sphere spinning impulsively. *Fluids* 2021; 6(6): 197. doi: 10.3390/fluids6060197
22. Chamkha AJ, Armaghani T, Mansour MA, et al. MHD convection of an $Al_2O_3$–Cu/water hybrid nanofluid in an inclined porous cavity with internal heat generation/absorption. *Iranian Journal of Chemistry and Chemical Engineering* 2022; 41(3): 936–956. doi: 10.30492/IJCCE.2021.136201.4328
23. Salahuddin T, Bashir AM, Khan M, et al. Hybrid nanofluid analysis for a class of alumina particles. *Chinese Journal of Physics* 2022; 77: 2550–2560. doi: 10.1016/j.cjph.2021.11.012
24. Reddy PS, Sreedevi P, Chamkha AJ. Hybrid nanofluid heat and mass transfer characteristics over a stretching/shrinking sheet with slip effects. *Journal of Nanofluids* 2023; 12: 251–260. doi: 10.1166/jon.2023.1996
25. Salahuddin T, Siddique N, Khan M, Chu YM. A hybrid nanofluid flow near a highly magnetized heated wavy cylinder. *Alexandria Engineering Journal* 2022; 61(2): 1297–1308. doi: 10.1016/j.aej.2021.06.014
26. Rashad AM, Chamkha AJ, Ismael MA, Salah T. Magnetohydrodynamics natural convection in a triangular cavity filled with a Cu–$Al_2O_3$/water hybrid nanofluid with localized heating from below and internal heat generation. *Journal of Heat Mass Transfer* 2018; 140(7): 072502. doi: 10.1115/1.4039213
27. Khan WA, Sun H, Shahzad M, et al. Importance of heat generation in chemically reactive flow subjected to convectively heated surface. *Indian Journal of Physics* 2021; 95: 89–97. doi: 10.1007/s12648-19-01678-2
28. Khan WA, Waqas M, Chammam W, et al. Evaluating the characteristics of magnetic dipole for shear-thinning Williamson nanofluid with thermal radiation. *Computer Methods and Programs in Biomedicine* 2020; 191: 105396. doi: 10.1016/j.cmpb.2020.105396
29. Khan WA, Ali M, Shahzad M, et al. A note on activation energy and magnetic dipole aspects for cross nanofluid subjected to cylindrical surface. *Applied Nanoscience* 2020; 10: 3235–3244. doi: 10.1007/s13204-019-01220-0
30. Khan WA, Ali M, Irfan M, et al. A rheological analysis of nanofluid subjected to melting heat transport characteristics. *Applied Nanoscience* 2020; 10: 3161–3170. doi: 10.1007/s13204-019-01067-5
31. Bejan A. A study of entropy generation in fundamental convective heat transfer. *Journal of Heat and Mass Transfer* 1979; 101(4): 718–725. doi: 10.1115/1.3451063
32. Mansour MA, Siddiqa S, Reddy Gorla RS, Rashad AM. Effects of heat source and sink on entropy generation and MHD natural convection of a $Al_2O_3$–Cu/water hybrid nanofluid filled with square porous cavity. *Thermal Science and Engineering Progress* 2018; 6: 57–71. doi: 10.1016/j.tsep.2017.10.014
33. Barman T, Roy S, Chamkha AJ. Entropy generation analysis of MHD hybrid nanofluid flow due to radiation with non-erratic slot-wise mass transfer over a rotating sphere. *Alexandria Engineering Journal* 2023; 67: 271–286. doi: 10.1016/j.aej.2022.12.051
34. Khan I, Khan WA, Qasim M, et al. Thermodynamic analysis of entropy generation minimization in thermally dissipating flow over a thin needle moving in a parallel free stream of two Newtonian fluids. *Entropy* 2019; 21(1): 74. doi: 10.3390/e21010074
35. Khan S, Ali F, Khan WA, et al. Quasilinearization numerical technique for dual slip MHD Newtonian fluid flow with entropy generation in thermally dissipating flow above a thin needle. *Scientific Reports* 2021; 11: 15130. doi: 10.1038/s41598-021-94312-3
36. Chamkha AJ, Rashad AM, Armaghani T, Mansour MA. Effects of partial slip on entropy generation and MHD combined convection in a lid-driven porous enclosure saturated with a Cu-water nanofluid. *Journal of Thermal Analysis and Calorimetry* 2018; 132(2): 1291–1306. doi: 10.1007/s10973-017-6918-8
37. Khan WA, Waqas M, Kadry S, et al. On the evaluation of stratification based entropy optimized hydromagnetic flow featuring dissipation aspect and Robin conditions. *Computer Methods and Programs in Biomedicine* 2020; 190: 105347. doi: 10.1016/j.cmpb.2020.105347